Nematic–lamellar tricritical behavior and structure of the lamellar phase in the ammonium pentadecafluorooctanoate (APFO)/water system

N. Boden, J. Clements, K. W. Jolley, D. Parker, and M. H. Smith

Citation: The Journal of Chemical Physics **93**, 9096 (1990); doi: 10.1063/1.459200
View online: http://dx.doi.org/10.1063/1.459200
View Table of Contents: http://scitation.aip.org/content/aip/journal/jcp/93/12?ver=pdfcov
Published by the AIP Publishing

Nematic–lamellar tricritical behavior and structure of the lamellar phase in the ammonium pentadecafluorooctanoate (APFO)/water system

N. Boden and J. Clements
School of Chemistry, University of Leeds, Leeds LS2 9JT, United Kingdom

K. W. Jolley
Department of Chemistry and Biochemistry, Massey University, Palmerston North, New Zealand

D. Parker[a)]
School of Chemistry, University of Leeds, Leeds LS2 9JT, United Kingdom

M. H. Smith
Department of Chemistry and Biochemistry, Massey University, Palmerston North, New Zealand

(Received 2 July 1990; accepted 11 September 1990)

^{2}H NMR spectroscopy has been used to map a high-resolution ($\pm$ 0.04 K) phase diagram for the ammonium pentadecafluorooctanoate(APFO)/heavy water system. It is qualitatively similar to that for the CsPFO/heavy water system. In particular, it exhibits a discotic micellar nematic phase N_D^+ intermediate to an isotropic micellar solution phase I and a lamellar phase for weight fractions of APFO between 0.395 ($\phi = 0.278$) and 0.589 ($\phi = 0.455$) and temperatures between 292.10 and 338.10 K. The N_D^+ to lamellar transition crosses over from second to first order behavior at a tricritical point similar to the superfluid transition in ^{3}He/^{4}He mixtures. X-ray scattering experiments show there to be no dramatic change in the structure of the micelle at the I to N_D^+ and the N_D^+ to lamellar transitions. Nematic order parameters (orientational order parameters of the discoidal micelles) have been calculated from electrical conductivity measurements. Their variation with temperature in the nematic phase and across the nematic to lamellar transition are qualitatively consistent with the behavior expected for thermotropic calamitic liquid crystals undergoing an isotropic to nematic to smectic-A sequence of transitions. It is, therefore, concluded that the transition from the N_D^+ to the lamellar phase solely involves the propagation of long range positional ordering of the discoidal micelles into planes along the nematic director, that is, the lamellar phase is a *discotic lamellar* phase L_D. This result reinforces previous claims about the structure of the lamellar phase of the CsPFO system as opposed to the alternative scenario of a classical lamellar phase in which the bilayers are perforated by microscopic defects. This conclusion is supported by measurements of ^{2}H quadrupole splittings of heavy water. Similar measurements for deuterated ammonium ions show a preference for counterion binding to sites of lowest surface curvature. The fraction of counterions bound to the surface of the micelle is shown to increase as the temperature is lowered due to a growth in diameter and associated changes in surface curvature.

I. INTRODUCTION

The classical soaps and soap-like surfactants, on dissolution in water, tend to form micelles in dilute solution[1] and liquid crystals, with extended aggregate structures, in concentrated solution.[2] The phase behavior is essentially universal[3] irrespective of the structure of the polar head group. The dominant features are that all of the phases are translationally ordered and the phase transitions are associated with a dramatic change in the topology of the aggregate. In contrast, it has fairly recently been recognized that with appropriate surfactants small discrete micelles can be stable at high concentrations where they form nematic phases.[4] These phases are characterized by long range correlations in the orientation of the micellar axes. Rod-shaped micelles form "canonic" phases N_C, disk shaped micelles, "discotic" phases N_D, and unsymmetric lath-like micelles, "biaxial" phases N_B. The nature of the isotropic-to-nematic transition is fairly well established, but the transition from the nematic to the smectic (translationally ordered) phase is not. The general perception is that this will involve a dramatic change in aggregate structure, viz. discoidal micelles into the infinite bilayers of lamellar phases or canonic micelles into the infinite cylinders of hexagonal phases. Indeed, current statistical mechanical models[5] predict that coupling between the size and the long-range orientational ordering of the micelles in the nematic phase leads to their "explosive" growth. However, the factors which govern the size and shape of micelles and the nature of the forces between them in concentrated solutions are not understood. At the present time there seems to be no *a priori* reasons why for appropriate surfactant systems sequential order–disorder transitions should not occur.

The evidence to date comes from studies of the N_D to lamellar transition in mainly the decylammonium chloride (DACl)/NH_4Cl/water[6] and the cesium pentadecafluorooctanoate (CsPFO)/water[7] systems. In the case of the binary DACl/water system, a N_D^- phase (the superscript de-

[a)] Present address is Department of Chemistry and Biochemistry, Massey University, Palmerston North, New Zealand.

 0021-9606/90/249096-10$03.00

notes the phase has negative diamagnetic susceptibility anisotropy) occurs intermediate to an isotropic micellar phase and a lamellar phase for DACl weight fractions w between 0.42 and 0.49. The nematic range is greatly enhanced by the addition of salt; indeed, until recently, it was believed that salt was essential to obtain a nematic phase with this system and this explains why all previous structural studies have been conducted on the ternary system. The lamellar to nematic transition appears to be continuous as no biphasic region is seen under the microscope. There is little variation of the electrical conductivity[8] in the direction of the nematic director on cooling into the lamellar phase suggesting that the lamellae are perforated by holes or microscopic defects or are layers of discrete discoidal micelles. X-ray scattering patterns[9,10] show a diffuse Bragg reflection corresponding to in-plane structure with a characteristic distance ($\approx$6.0 nm) of the order of the side-to-side separation of the micelles in the nematic phase: this has been interpreted in terms of a perforated bilayer which inverts to discoidal micelles at the nematic-to-lamellar transition. However, freeze-fracture transmission electron micrographs[11] indicate that discrete micelles persist well into the lamellar phase. In the CsPFO/^2H_2O system, a N_D^+ phase is formed over a wide concentration interval without addition of salt: it occurs for w between 0.225 ($\phi = 0.114$) and 0.632 ($\phi = 0.426$) and temperatures T between 285.3 and 351.2 K. The N_D^+ to lamellar transition is characterized by a tricritical point (Tcp: $w = 0.43$ ($\phi = 0.25$); $T = 304.80$ K[12]), analogous to the ^{3}He/^{4}He superfluid transition. Its origin has been explained by inclusion of both anisotropic repulsive and attractive terms into the McMillan model[13] for the nematic to smectic-A transition in thermotropic calamitic liquid crystals. The x-ray scattering patterns[14,15] electrical conductivity,[14,16] and NMR measurements[7] are consistent with there being no significant change in either the shape or size of the discoidal micelles at the transition. Furthermore, the variation with temperature and the actual values of the orientational order parameters of the micelles are also in accord with the McMillan model.[13] Thus, in the case of the CsPFO/water system and very likely for the DACl/NH_4Cl/water system, too, it seems reasonable to conclude that the lamellar phase is comprised of discoidal micelles arranged on equidistant planes. This *discotic lamellar phase* is denoted L_D.

A recent electrical conductivity and density study performed on both the CsPFO/water and the DACl/NH_4Cl/water systems,[17] argues for a "classical" bilayer structure for the lamellar phase. The conductivity measurements can, however, be equally well explained in terms of textural distortions in an L_D phase caused by heating, together with a slow reorientation of the director along the magnetic field as a result of pretransitional fluctuations close to the L_D to N_D^+ phase transition temperature.[18] Moreover, any conclusions based on the density measurements of this and a previous study,[19] must be treated with caution since the measurements show a negative ΔV at both the L_D to N_D^+ and the N_D^+ to I transitions. It has been shown that both dT_{NI}/dp[20] and ΔH[7] for the latter transition are positive and ΔV should, therefore, be small and positive.[20] The observation of a relatively large, negative ΔV is probably the result of the generation of bulk defects as a consequence of surface alignment in the narrow capillary of the vibrating densitometer employed in the density measurements.

The existence of N_D^+ phases has also been reported for cesium,[21] ammonium,[22,23] and tetramethylammonium[23] heptadecafluorononanoate (HFN)/water systems, but there is uncertainty as to the nature of the nematic to lamellar transitions and structures of their lamellar phases. The available phase diagrams do not distinguish between first and second order nematic to lamellar transitions. From electrical conductivity measurements[24] and NMR measurements of water self-diffusion coefficients[25] in the AHFN/water system, it has recently been concluded that in the lamellar phase the lamellae are perforated bilayers. In contrast, the small angle neutron scattering patterns[26] for the TMAHFN/water system are quite similar to those obtained by x rays for the CsPFO/water system and seemingly suggest the lamellae are comprised of discrete discoidal micelles. Clearly, there is a need to establish whether or not all lamellar phases which are conjugate to N_D phases are of the type L_D or whether in some cases they may be classical bilayer phases. To this end, we report a study of the phase behavior and structure of the ammonium pentadecafluorooctanoate(APFO)/water system. A previous study[27] on this system has established the existence of a lamellar phase, though a nematic phase was not evident. The high resolution phase diagram reported herein is delineated by NMR spectroscopy, the structure of the aggregates is established by x-ray scattering and supported by NMR measurements, and the orientational order parameters of the micelles are calculated from electrical conductivity measurements. All of the results are shown to be consistent with a discotic lamellar phase.

II. METHODS

APFO was prepared by neutralizing an aqueous solution of pentadecafluorooctanoic acid (Fluorochem Ltd.) with ammonium hydroxide. The neutral solution was freeze dried and the salt was recrystallized from a 10:1 (v/v) *n*-hexane/*n*-butanol solution. Samples were made up in D_2O (Aldrich).

The phase diagram was mapped using ^{2}H NMR spectroscopy of labeled water as described elsewhere[7] for the CsPFO system. Spectra were measured with a JEOL GX270 spectrometer operating at 41.45 MHz. The temperature of the sample was controlled and measured to within 5 mK.

X-ray scattering experiments were conducted with a simple pinhole camera, nickel-filtered Cu K_α radiation of wavelength $\lambda = 0.154$ nm, Lindemann sample tube (0.5 mm i.d.) to plate distance of 113.5 mm, and with a 0.4 T magnetic field parallel to the z axis (equator) and perpendicular to the x axis (meridian) which is the direction of the long axis of the Lindemann tube.

The electrical conductivity measurements were made with a HP 4192a impedance analyzer (5 Hz–13 MHz). Readings were taken at 100 mK intervals on cooling the sample from the isotropic, through the nematic, into the la-

mellar phase. The conductivity cell comprised a pair of platinized platinum foil 1×1 cm squares mounted 1 cm apart. In both the x-ray and conductivity experiments the temperature of the sample was controlled and measured to the same precision as in the NMR experiments.

III. RESULTS AND DISCUSSION

A. Phase diagram and tricritical point

A partial phase diagram is given in Fig. 1 (The full phase diagram and a description of its delineation will be presented elsewhere). It shows an N_D^+ phase intermediate to an isotropic micellar solution phase I and what will herein be demonstrated to be a L_D phase. The N_D^+ phase is seen to be stable between w of 0.395 ($\phi = 0.278$) and 0.589 ($\phi = 0.455$) and temperatures of 292.1 and 338.1 K. This is a little less extensive than in the CsPFO system, but otherwise the phase diagrams are very similar: Indeed, in T vs ϕ coordinates the phase diagrams are almost identical except that the corresponding transition temperatures are some 23 K higher for the CsPFO system. The lamellar–nematic tricritical point Tcp is fixed at $w = 0.490$ ($\phi = 0.362$) with a corresponding temperature of 304.0(1) K. This should be taken as an upper limit in view of the intrinsic limitation in the resolution of the deuterium NMR signals from coexisting N_D^+ and L_D phases. ^{133}Cs NMR, which has at least an order of magnitude greater resolving power, was used to locate Tcp in the CsPFO system.[12] It was not practicable to use the ^{14}N resonance of the ammonium ion in this way because the advantages of the larger quadrupole splittings for ^{14}N as compared to ^{2}H are offset by the larger linewidths. For the $w = 0.451$ sample at T_{LN} (296.32 K) the ^{14}N splitting is 34 660 Hz as compared with 702 Hz for the ^{2}H splitting, and the linewidths are 400 and 5 Hz, respectively. The other singular points to note are the critical end point Cep [$T = 292.4(1)$ K, $w = 0.430$ ($\phi = 0.308$)] where the line of second order L_D to N_D^+ transitions intersect the solubility curve T_c, the $I/N_D^+/L_D$ triple point [$T = 338.10(5)$ K, $w_I = 0.581$ ($\phi = 0.446$), $w_N = 0.589$ ($\phi = 0.455$), and $w_L = 0.604$ ($\phi = 0.470$)], and the $I/N_D^+/K$ triple point [$T = 292.1(1)$ K, $w_I = 0.393$ ($\phi = 0.277$), $w_N = 0.395$ ($\phi = 0.278$), $w_K = 1.0$].

The most interesting feature of the phase diagram is the occurrence of the tricritical point at which the L_D to N_D^+ transition crosses over from second to first order behavior, similar to the superfluid transition in ^{3}He/^{4}He mixtures. This is precisely the phase behavior predicted by McMillan[13] and De Gennes[28] for the smectic-A to nematic transition in thermotropic calamitic liquid crystals and subsequently observed in binary mixtures.[29–32] In these systems second order transitions are usually associated with a wide nematic range and first order transitions with a narrow nematic range such that the width of the nematic phase increases as one moves further away from the tricritical point. In contrast, in the APFO system, T_{LN}/T_{NI} is 0.9800 (cf. 0.9815 in the CsPFO system) at Tcp and is essentially invariant along the line of second order transitions and the nematic domain is unusually narrow (6 K).

The existence of the lamellar–nematic tricritical point indicates that the I to N_D^+ to L_D sequence of transitions is quite analogous to the isotropic liquid to nematic to smectic-A sequence observed for thermotropic calamitic liquid crystals.[13] This suggests that the transition is a simple order–disorder one and does not involve any significant change in the structure of the micelles. This assertion is tested below by analysis of electrical conductivity and NMR measurements for samples with a nominal concentration w of 0.45 (i.e., the transition is second order).

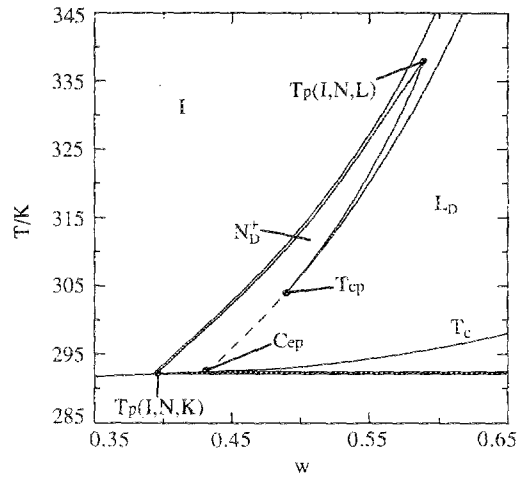

FIG. 1. Partial phase diagram of the APFO/D_2O system showing the isotropic micellar solution phase I, the nematic phase N_D^+, and the discotic lamellar phase L_D. All unlabeled areas are biphasic regions. The temperatures of the phase boundary curves are estimated to have errors of ± 0.04 K.

B. X-ray scattering experiments

The scattering pattern for a sample with $w = 0.452$ in the isotropic phase is a single diffuse ring [Fig. 2(a)]. On cooling into the nematic phase, in the presence of a magnetic field, the observed scattering pattern displays considerable anisotropy [Fig. 2(b)] consistent with the onset of long range orientational ordering. The intense Bragg peak along the meridian (x) arises from the "face-to-face" separation $d_\parallel$ of the micelles parallel to the nematic director. The weaker diffuse scattering along the equator (z) arises from the "side-to-side" separation $d_\perp$ of the micelles in the plane perpendicular to the director. Thus the nematic phase must be of the N_D^+ type. The nematic phases of the CsPFO[14] and the DACl[9,10] systems give similar diffraction patterns except that in the latter case the pattern is rotated through 90° as it is of the N_D^- type.

As the nematic phase is further cooled, both positional and orientational order increase as is indicated by the sharpening of the Bragg peak along the meridian and the reduction in the azimuthal extent of the Bragg peak [Fig. 2(c)]. At the nematic to lamellar transition there is no discernible change in the scattering pattern [Fig. 2(d)]. The transition appears simply to involve the onset of long range positional ordering of the micelles along the direction of the nematic director without any dramatic change in their structure. The absence of any observable change in the scattering intensity along the equator, is consistent with the persistence of liquid-like disorder, in the plane normal to the nematic director, into the lamellar phase. That is, the lamellar phase is of type

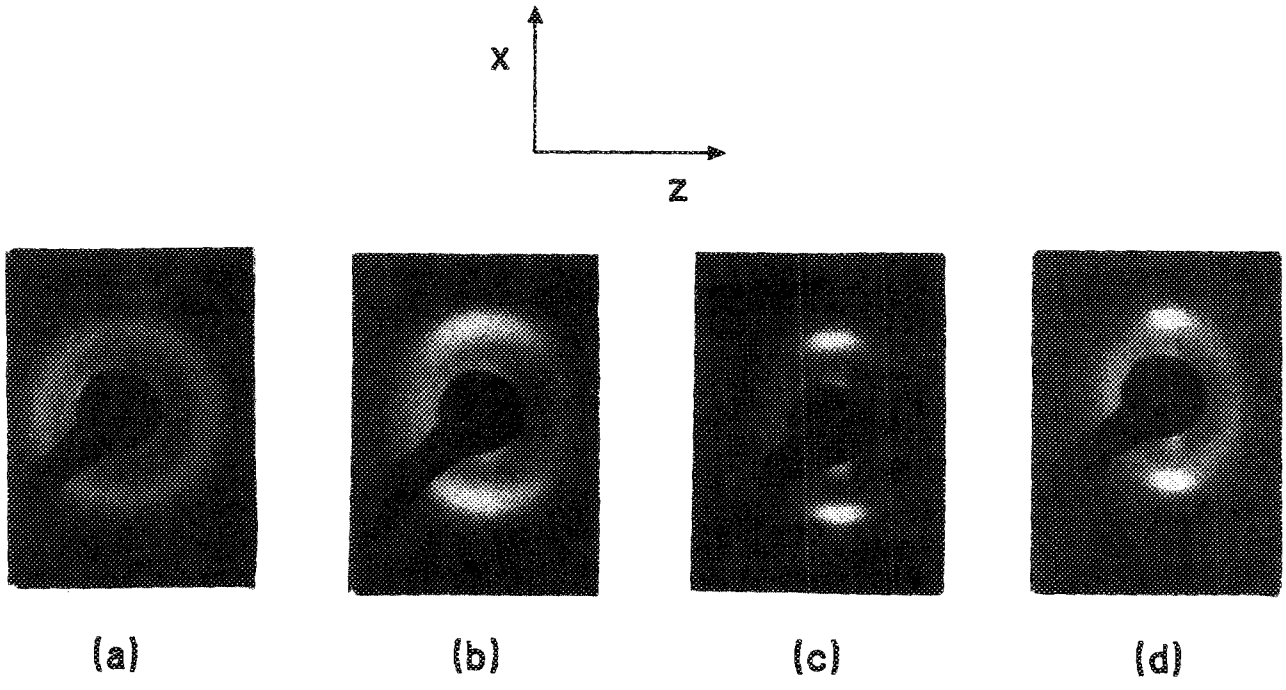

FIG. 2. X-ray scattering patterns of APFO/D_2O ($w = 0.452$): $T_{LN} = 296.70$ K, $T_{NI} = 302.70$ K, and $T_{IN} = 303.18$ K. (a) I phase at 309 K, (b) N_D^+ phase at 302 K, (c) N_D^+ phase at 299 K, (d) L_D phase at 296 K.

L_D. The corollary of this interpretation is that local positional organization of the micelles in the L_D phase persists into the nematic phase. This behavior is in direct contrast to that observed in thermotropic calamitics which exhibit a discontinuous change in the x-ray scattering pattern at the nematic to smectic-A transition.[33] Furthermore, for thermotropic calamitics at temperatures just above the nematic to isotropic transition, the x-ray diffraction pattern shows two diffuse rings indicative of short range positional and orientational correlations of the *molecules* in the isotropic phase. However, in these micellar systems the existence of only a single diffuse diffraction ring suggests that such correlations are much weaker. There are two possible explanations for this observation. Either the micelles undergo uncorrelated orientational fluctuations, consistent with their low volume fraction, or they change from discoidal to spherical aggregates at the nematic to isotropic transition. To distinguish between these two possibilities requires an estimation of aggregation numbers.

In view of the pseudolamellar structure of the nematic phase, it seems reasonable to assume the discoidal micelles are hexagonally packed into planes with separation $d_\parallel$ and separation of the (11) planes corresponding to $d_\perp$. The volume V_m of the micelle can then be calculated from[14] $V_m = 2d_\parallel d_\perp^2 \phi/\sqrt{3}$ and hence the average aggregation number $\tilde{n}$ from $\tilde{n} = V_m/V_S$,[34] where $V_S = 0.383$ nm^3. The same procedure is applicable in the L_D phase, while in the isotropic phase it is a reasonable approximation to assume that the x rays are scattered from the (111) planes of a fcc lattice with separation d_0, such that $V_m = 3\sqrt{3}\phi d_0^3/4$. The aggregation numbers calculated in this manner from the d spacings in Fig. 3(a) are summarized in Fig. 3(b).

There is an apparent decrease in the aggregation number from 119 to 100 at the nematic to isotropic transition. This could arise from the change of model. However, as will be shown below, conductivity measurements also predict a similar abrupt change in aggregation number. Thus, we can conclude the micelles in the isotropic phase are far too large to be consistent with the aggregation number of 18 estimated for a classical spherical micelle composed of PFO^- ions.[35]

The interpretation of both electrical conductivity and NMR measurements requires the assumption of an analytical shape for the micelle. An oblate ellipsoid is chosen as the simplest and most plausible, and also because it was found to be the most appropriate for the CsPFO/water system.[14] The length of the minor axis a of 2.2 nm, as used for the CsPFO system,[36] will be shown to be consistent with the results for APFO, too. The corresponding value for the axial ratio a/b are given in Fig. 3(b).[37] The values for the diameter b can be compared with the center-to-center separation of the micelles calculated assuming a close packed arrangement for the micelles. These are, respectively, 6.11 and 6.04 at T_{NI}, 6.62 and 6.46 at T_{NL}, and 7.26 and 7.04 at 290 K. Thus, there is an apparent agreement with the model of close packed micelles in layers. The CsPFO system was found to behave identically.[14] Moreover, at the nematic to isotropic transi-

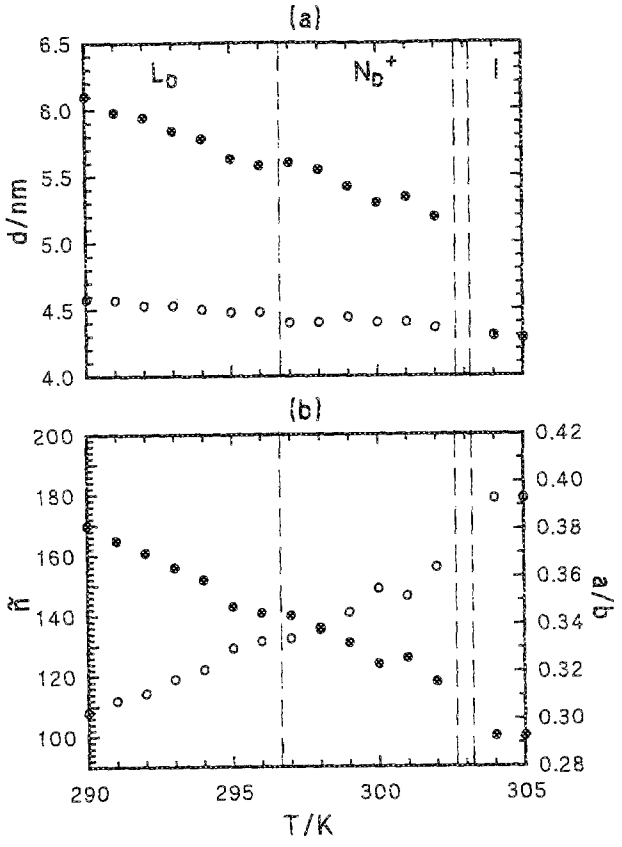

FIG. 3. (a) d spacings calculated from the maxima in the intensity of the scattering curves in Fig. 2 using Bragg's law: $d_{\|}$ (●) is the face-to-face separation of the micelle measured along the meridian, $d_{\perp}$ (○) is the side-to-side separation measured along the equator, and d_0 (◑) is the average center-to-center separation measured in the isotropic phase. (b) Average aggregation numbers $\tilde{n}$(●) and axial ratios a/b(○) (assuming $a = 2.2$ nm) of discoidal micelles calculated as described in the text.

tion the reduced density $\rho^*_{NI} = \rho b^3$ is 1.59 as compared with the value 1.67 obtained in the CsPFO system at similar concentrations.[15]

The most notable features of the data in Fig. 3(b) are the discontinuity in the aggregation number at the isotropic to nematic transition and its temperature dependence. Statistical mechanical models[5] predict a similar increase in the size of the micelles at this transition, which is purported to be driven by the entropy loss arising from the establishment of long range orientational order. The system attempts to minimize this loss of entropy by making the micelles larger, i.e., there are fewer micelles to lose entropy. Similarly, the greater rate of increase of micelle size in the nematic phase is in keeping with the expected increase in the orientational order. However, there is no evidence for the predicted divergence in the rate of growth due to the coupling of the micelle size to the nematic order parameter.[5] The continuous growth in micelle size in the lamellar phase suggests that the micelle size is also coupled to the translational order of the smectic phase. Thus there is a need to extend the earlier statistical mechanical theories for micellar solutions to include these newer observations.

C. Electrical conductivity measurements and orientational ordering of the micelles

One way to test the model proposed for the structure of the nematic and lamellar phases is to compare the temperature dependence of the nematic orientational order parameter S of the micelle with the behavior predicted[13] for the isotropic to nematic to smectic transitions in thermotropic calamitic liquid crystals. S is defined by $\langle P_2(\cos\beta)\rangle$ where β is the angle between the symmetry axis of the micelle and the mesophase director $\hat{n}$ and the angular brackets denote an ensemble average. Measurements of any second rank property may in principle be used to obtain values for S. The molecular properties usually used for this purpose will, however, contain contributions from the reorientational motion of the surfactant molecules within the micelle and these will change with the size of the micelle. Thus, they cannot provided absolute values for S. It turns out, quite remarkably, that electrical conductivity measurements can be used for this purpose;[14,38] the procedure is justified elsewhere.[36] It is practicable because the conductivity is solely determined by the diffusivity of the counterions around the micelles. The contribution from the micelles is negligible at these high concentrations as their diffusive motion is hindered by strong intermicellar interactions.

For nonconducting, ellipsoidal micelles undergoing reorientational fluctuations with respect to the director of a uniaxial mesophase, the conductivity transforms as a second rank tensor with a principal axes system coincident with that of the moment of inertia tensor. The experiment, therefore, measures the partially averaged component $\tilde{\kappa}_{zz}$ of the conductivity tensor along the direction of E which is taken to be along the z axis of the laboratory frame $L(x,y,z)$. This is given by

$$\tilde{\kappa}_{zz}(\phi) = \kappa_i + \tfrac{2}{3}P_2(\cos\phi)S(\kappa_{\|} - \kappa_{\perp})_M, \qquad (1)$$

where ϕ is the angle between the mesophase director and the direction of E. κ_i is the trace of the conductivity tensor κ as measured in the isotropic phase ($S = 0$) and in the liquid crystalline phases when $\phi = 54°\ 44'$ [i.e., $P_2(\cos\phi) = 0$]. $(\kappa_{\|})_M$ and $(\kappa_{\perp})_M$ are the conductivities measured parallel and perpendicular to the micellar symmetry axis in the micelle frame $M(a,b,c)$ and may be interpreted as $\tilde{\kappa}_{zz}(0°)$ and $\tilde{\kappa}_{zz}(90°)$ in a perfectly ordered system ($S = 1$). From Eq. (1),

$$\Delta\tilde{\kappa}/\kappa_i = S(\kappa_{\|} - \kappa_{\perp})_M/(\kappa_{\|}/3 + 2\kappa_{\perp}/3)_M, \qquad (2)$$

where $\Delta\tilde{\kappa} = \tilde{\kappa}_{zz}(0°) - \tilde{\kappa}_{zz}(90°)$. The conductivity measurements for a sample with $w = 0.447$ are summarized in Fig. 4(a). We see that in the nematic phase $\tilde{\kappa}_{zz}(0°) < \tilde{\kappa}_{zz}(90°)$, consistent with it being a N_D^+ phase. The absence of any discernible discontinuities at the N_D^+ to L_D transition is also consistent with the phase diagram and the x-ray diffraction measurements. It supports the notion of discoidal micelles undergoing a second order transition to a L_D phase. There is seen to be a small decrease in the value of κ_i at the I to N_D^+ transition. This corresponds to an increase of 14% in the

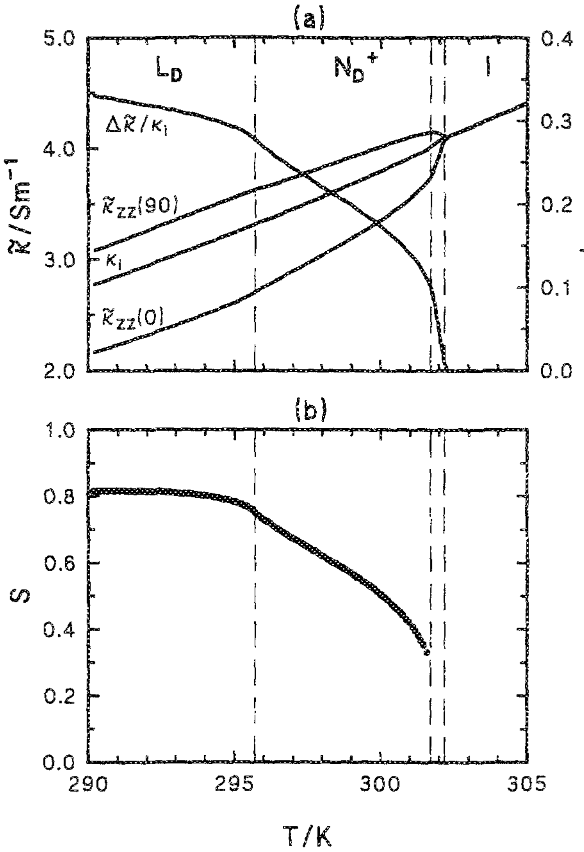

FIG. 4. (a) The electrical conductivity $\tilde{\kappa}_{zz}(\phi)$ as a function of temperature as measured at 30 kHz for APFO/D_2O with $w = 0.447$ ($T_{LN} = 295.70$ K, $T_{NI} = 301.71$ K, and $T_{IN} = 302.18$ K). $\tilde{\kappa}_{zz}(0°)$ and $\tilde{\kappa}_{zz}(90°)$ are the conductivities measured parallel and perpendicular to the lamellar/nematic director, while κ_i corresponds to $\tilde{\kappa}_{zz}(54° 44')$ in the nematic and lamellar phases. The relative conductivity anisotropy is $\Delta\tilde{\kappa}/\kappa_i = \{\tilde{\kappa}(0°) - \tilde{\kappa}(90°)\}/\kappa_i$. (b) Temperature dependence of the orientational order parameter S as calculated from Eq. (2).

micelle aggregation number and is in good agreement with the increase of 19% suggested by the model dependent x-ray results in Fig. 3(b).

Equation (2) has been employed to obtain values of S from the conductivity measurements in Fig. 4(a) using values of $(\kappa_{\parallel})_M$ and $(\kappa_{\perp})_M$ calculated[14,36] from the micelle dimensions in Fig. 3(b). To do this it was necessary to combine the data from the conductivity and x-ray experiments. Since the samples used in these experiments have slightly different concentrations ($w = 0.447$ and 0.452 for the conductivity and x-ray samples, respectively), the data were matched by normalizing the measured temperatures for the two experiments to their respective T_{NI} values. This was also the technique used to compare the NMR experiments (sample weight fraction $w = 0.451$) with the conductivity and x-ray experiments (Sec. III D). The values of S so obtained are summarized in Fig. 4(b). The behavior at the nematic to lamellar transition is exactly as predicted by the McMillan model[13] for a second order transition, as is the value of S (0.75) at T_{NL}. The downward turn in S on the lamellar side of the transition and the upwards turn on the nematic side are indicative of strong pretransitional effects. Indeed, on the lamellar side of the transition we find from our NMR experiments, that the director rotates into alignment along the direction of the magnetic field for $(T_{LN} - T) < 0.5$ K. The value of S at T_{NI} is 0.28 as compared with the mean field value of 0.43, but the values for thermotropics are also lower. Again we note a strong downward turn in S on approaching the transition, indicative of strong pretransitional effects. Fitting data to the power law $S - S^+ = A(T^+ - T)^{\beta}$ where S^+ is the order parameter at T^+, the superheating limit of the nematic phase, gave $\beta = 0.34 \pm 0.01$, $S^+ = 0.06 \pm 0.05$, and $T^+ - T_{NI} = 0.19 \pm 0.01$ K. This value of β is to be compared with that obtained[39] (0.34 ± 0.06 at $w = 0.398$) for the CsPFO/H_2O system.

The relatively weak temperature dependence of S in the L_D phase is characteristic of thermotropic smectic-A phases, but the temperature dependence in the N_D^+ phase is more dramatic than the near universal behavior[40] of thermotropic nematic phases. This behavior and the narrow nematic range (typically 6 K) have their origin in the growth in size of the micelle as the temperature of the nematic phase is lowered. This can be seen by considering the modified Maier–Saupe[41] expression for the nematic to isotropic transition temperature: $T_{NI} = (0.2202/k)\varepsilon_{mm}\phi/V_m$, where ε_{mm} is the strength of the anisotropic dispersive interaction between the micelles. Now, for a discoidal micelle it is plausible to expect that $\varepsilon_{mm} \propto \tilde{n}^2$ so that $T_{NI} \propto \tilde{n}\phi$. Thus, the growth of the micelle as the temperature is lowered *accelerates* the nematic phase to lower reduced temperatures until the nematic order parameter attains the value at which the transition to the lamellar phase is initiated. That is, the nematic phase is a compressed version of what it would be if the size of the micelle was invariant. This behavior highlights a fundamental difference between micellar mesophases and their thermotropic counterparts.

The nematic order parameter has also been calculated from the angular intensity distribution $I(\Psi)$ of the meridional reflection (Fig. 2) where Ψ is the angle between the radius vector and the x axis. The values so obtained are, as for the CsPFO system,[14] significantly larger than those obtained from conductivity measurements. All the micellar nematic phases so far investigated[9,10,14,42-44] behave similarly: S varies between 1.0 and 0.7. Thus, the order parameters obtained from x-ray measurements seem anomalously high. Yet the x-ray method has given reasonable values for thermotropic nematic phases[33] although justifiably criticized.[45] The discrepancy between the values of the order parameters as obtained by the two techniques must have its origin in the different ways in which they sense the reorientational fluctuations of the micelles. The order parameters obtained from the electrical conductivity measurements represent the ensemble average of the orientational fluctuations of the micellar axes $M(a,b,c)$ with respect to the laboratory frame $L(x,y,z)$ over a time scale determined by the measurement period (typically, 3×10^{-5} s). Now, in contrast, the angular intensity distribution $I(\Psi)$ in the meridional reflection of the x-ray diffraction pattern represents the instantaneous ensemble average orientational distribution of the intermicellar vectors. This will not be affected by any independent

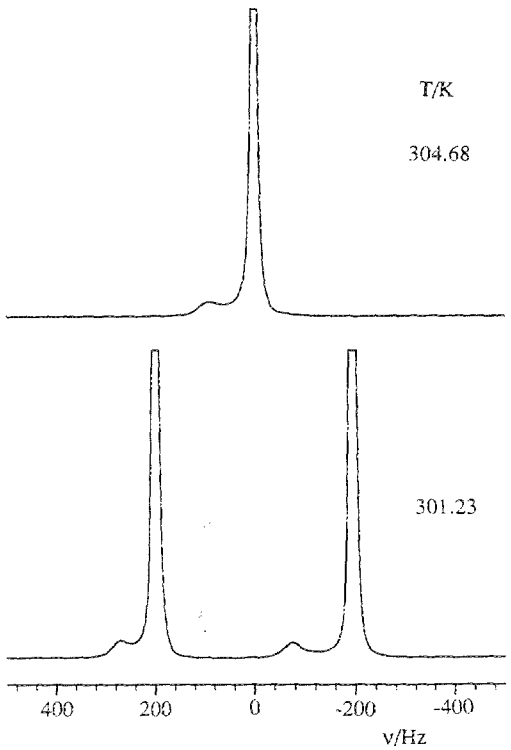

FIG. 5. ^{2}H NMR spectra as observed on cooling the sample APFO/D_2O ($w = 0.451$) from the I (top) into the N_D^+ phase (bottom). In the I phase spectrum the deuterated ammonium ion peak is clearly seen to high frequency (84 Hz) of the D_2O peak while in the N_D^+ phase both the deuterated ammonium ion and the heavy water show a quadrupole splitting. The D_2O peaks have been "cut off" for convenience of presentation but the intensities of the two signals are in the ratio of 13.4:1 which is to be compared with the expected ratio of heavy water to ammonium ion deuterons of 13.1:1.

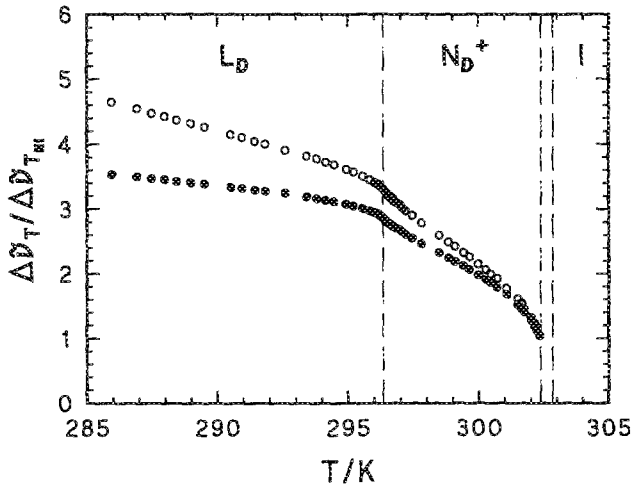

FIG. 6. Partially averaged ^{2}H quadrupole splittings $\Delta\tilde{\nu}$, normalized to their value at T_{NI}, as a function of temperature for APFO/D_2O ($w = 0.451$): $T_{LN} = 296.32$ K, $T_{NI} = 302.39$ K, and $T_{IN} = 302.85$ K. For D_2O (●), $\Delta\tilde{\nu}(T_{NI}) = 244$ Hz and for ND_4^+ (○), $\Delta\tilde{\nu}(T_{NI}) = 200$ Hz.

reorientational fluctuations of the individual micelles, which is very likely to be a significant reorientational mode in micellar nematic phases in view of the low packing fraction: that is the micelles are wobbling. The intensity distribution in the x-ray reflection derives from the longer range collective fluctuations.

D. ^{2}H NMR measurements

NMR measurements of quadrupole splittings in labeled water provide a microscopic probe of the micelle shape, size, and orientational order. As such they can provide a confirmation of the interpretation of the x-ray and conductivity measurements. Figure 5 shows the ^{2}H spectrum of a $w = 0.451$ sample in the I and N_D^+ phases. The high and low frequency peaks in the I phase are assigned, respectively, to ND_4^+ and D_2O on the basis of their relative intensities (1:13). This ratio is consistent with a statistical distribution of deuterium spins effected by chemical exchange between the ammonium ions and water molecules. The ND_4^+ peak, therefore, contains contributions from all the species $NH_nD_{4-n}^+$. The absence of scalar couplings $J_{^2H-^1H}$ (1.2 Hz) and $J_{^2H-^{14}N}$ (8.1 Hz)[46] shows that exchange of ^{2}H between these species must be faster than 50 s^{-1} ($2\pi J$). To observe these spin interactions would require a pH of about 1.0[46,47] as compared to the value 5.5 of our sample. The linewidths of the ND_4^+ and D_2O peaks are, respectively, 42 and 5 Hz and represent the combined contributions from spin–spin relaxation, chemical exchange between the ND_4^+ and D_2O peaks, and magnetic field inhomogeneities. For comparison, the corresponding linewidth for D_2O in the CsPFO system is only 2 Hz. If this is taken to be the combined contribution from spin–spin relaxation and magnetic field inhomogeneities, then the net contributions from chemical exchange to the observed linewidths of the ND_4^+ and D_2O peaks are, respectively, 40 and 3 Hz. These contributions can be identified with $(\pi\tau_A)^{-1}$ and $(\pi\tau_W)^{-1}$ where τ_A and τ_W are the mean lifetimes of a deuterium spin at, respectively, the ammonium and water sites. These quantities can be used to estimate a value for the mean time interval between successive transfers of a deuterium spin from the relationship $\tau = p_W\tau_A = p_A\tau_W$, where p_W ($= 0.929$) and p_A ($= 0.071$) are the fractional populations of the water and ammonium sites. This gives a value of 135 s^{-1} for τ^{-1}. On cooling into the N_D^+, and subsequently into the L_D phase, each resonance is seen to be spiit into a doublet and these splittings are plotted as a function of temperature in Fig. 6. The variation with temperature of both splittings is seen to reflect the behavior of the order parameter [Fig. 4(b)], though there are clearly other contributions especially for the ND_4^+ ion.

The partially averaged quadrupole splitting of ^{2}H in either D_2O or ND_4^+ is described by[7]

$$\Delta\tilde{\nu}(\phi) = \tfrac{3}{2}|\tilde{q}_{zz}|_s SP_2(\cos\phi), \tag{3}$$

where ϕ is the angle between the mesophase director $\hat{n}$ and the direction of the magnetic field H and has the value 0° in all of our experiments, and $|\tilde{q}_{zz}|$ is a parameter solely deter-

mined by the structure of the micelle. For D_2O,

$$|\tilde{q}_{zz}|_s = \langle P_2(\cos\alpha)\rangle_s \chi_D^W (x_S/x_W) n_b S_{OD}, \quad (4)$$

where χ_D^W is the quadrupole coupling constant for a water molecule, x_S and x_W are, respectively, the mole fractions of surfactant and water, n_b is the number of water molecules bound to each surfactant molecule, and S_{OD} is an "order parameter" representing the averaging due to the local reorientational motion of these water molecules. The quantity

$$\langle P_2(\cos\alpha)\rangle_s = \langle \tfrac{3}{2}\cos^2\alpha - \tfrac{1}{2}\rangle_s, \quad (5)$$

where α is the angle between the normal to the surface and the symmetry axis of the micelle and the angular brackets denote an average over the surface, accounts for the averaging due to the diffusive motion of a water molecule over the surface of a micelle. For molecules not bound to the surface $|\tilde{q}_{zz}|_s = 0$. Now, to a good approximation, all quantities other than S and $\langle P_2(\cos\alpha)\rangle_s$ in Eq. (3) are expected to be constant over the temperature interval of the measurements. We can therefore, write

$$\Delta\tilde{\nu}_T/\Delta\tilde{\nu}_{T_{NI}} = (S\langle P_2(\cos\alpha)\rangle_s)_T/(S\langle P_2(\cos\alpha)\rangle_s)_{T_{NI}}. \quad (6)$$

Thus, a plot of the quantity on the left-hand side vs the quantity on the right-hand side of Eq. (6) may be used to test whether the model invoked to account for the x-ray and conductivity measurements is appropriate. To do this values of $\langle P_2(\cos\alpha)\rangle_s$ have been calculated from the axial ratios of the micelle [Fig. 3(b)][7] and the results are plotted in Fig. 7. We see that over the temperature range T_{NI} to $T_{LN} - 5$ K the plot is indeed linear with a slope of unity [1.02(2)], consistent with the model. The shape of the plot of $\Delta\tilde{\nu}(D_2O)$ vs temperature in Fig. 6 can now be understood in terms of the temperature dependence of the two quantities S and $\langle P_2(\cos\alpha)\rangle_s$. The behavior in the N_D phase is clearly dominated by the temperature dependence of S, while in the L_D phase it is the temperature dependence of the shape factor which prevails. The excellent fit to the model also indicates that the interaction of water molecules with the micelle surface is not substantially altered by changes in the fraction of bound ammonium ions (see Fig. 8).

There must be an additional contribution to the temperature dependence of the quadrupole splittings of the ammonium ion. This arises from the variation with temperature of the fraction f_A of ammonium ions bound to the surface of the micelle. The expression for $|\tilde{q}_{zz}|_s$ is now

$$|\tilde{q}_{zz}|_s = \langle P_2(\cos\alpha)\rangle_s \chi_D^A f_A S_{ND}, \quad (7)$$

where χ_D^A is the quadrupole coupling constant for the ND_4^+ ion and S_{ND} is an "order parameter". For ND_4^+ ions not bound to the surface $|\tilde{q}_{zz}|_s = 0$, while the observation of a finite quadrupole splitting implies that those ions which are bound must be distorted from tetrahedral symmetry.[46] In the calculation of $\langle P_2(\cos\alpha)\rangle_s$ account must be taken of the fact that the distribution of ammonium ions over the surface is not expected to be uniform. It will be determined by the surface charge density which is anticipated to be greater the lower the radius of curvature for an oblate ellipsoidal micelle. Though there are no reported calculations to date for ion binding to such a micelle, the observed quadrupole splittings can be used to test the above hypothesis. This requires

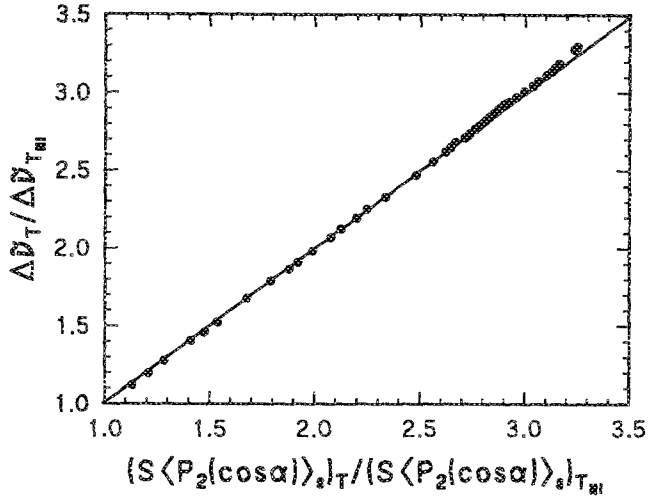

FIG. 7. Plot of Eq. (6). The straight line has a slope of one and an intercept of zero as predicted. The best fit values for these two quantities are 1.02(2) and −0.04(4), respectively.

values for f_A which we have calculated from the conductivity measurements using an expression first derived by Fricke.[48]

$$\kappa_i = \tfrac{1}{3}\kappa_0(1-\phi)(1-f_A) \times\left[\frac{2}{1-\phi(1+\beta_\perp)} + \frac{1}{1-\phi(1+\beta_\parallel)}\right]. \quad (8)$$

Here, $\beta_\parallel$ and $\beta_\perp$ are shape factors representing the obstruction by the micelle of counterion diffusion parallel and perpendicular to the micellar symmetry axis, respectively, which can be calculated from the axial ratio a/b. κ_0 is the conductivity of the continuous phase which is equal to

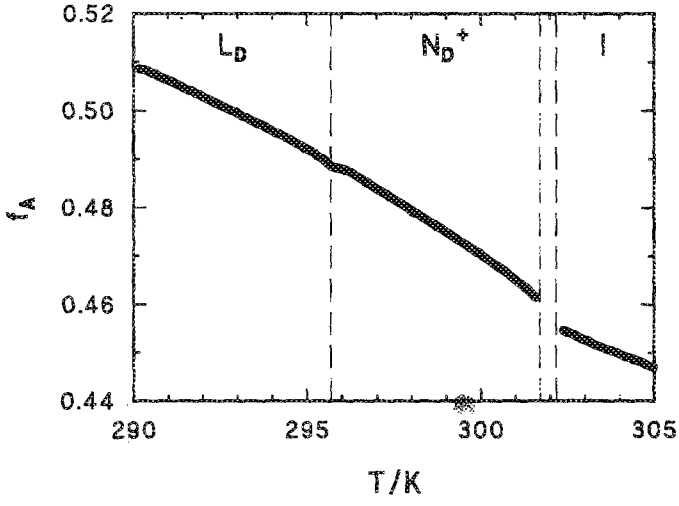

FIG. 8. Temperature dependence of f_A for APFO/D_2O ($w = 0.447$) as calculated from Eq. (8).

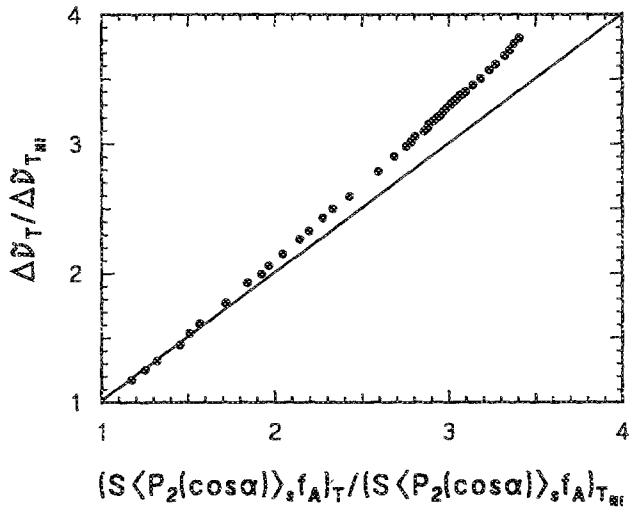

FIG. 9. Plot of Eq. (9). The straight line has a slope of one and an intercept of zero appropriate to a uniform distribution of ND_4^+ binding sites. The positive departure from Eq. (9) is due to preferential binding of ND_4^+ ions at sites with low surface curvature.

$c\lambda^0_{ND_4^+}$, where c is the ionic concentration and $\lambda^0_{ND_4^+}$ is the limiting molar conductivity of the ND_4^+ ions. Values for $\lambda^0_{ND_4^+}$ in heavy water at a given temperature were obtained by taking the corresponding value in H_2O[49] and multiplying it by the viscosity ratio $\eta(H_2O)$[50]$/\eta(D_2O)$[51] at that temperature. (The assumption implicit in this relationship, which is derived from the Stokes–Einstein equation, is that there is negligible change in the hydrodynamic radius of the ND_4^+ ions on replacing water with heavy water.) Equation (8) has been used to calculate values for f_A from the κ_i in Fig. 4(a); the results are summarized in Fig. 8. Now proceeding as for the quadrupole splittings of D_2O, that is writing

$$\Delta\tilde{\nu}_T/\Delta\tilde{\nu}_{T_{NI}} = (S\langle P_2(\cos\alpha)\rangle_s f_A)_T/(S\langle P_2(\cos\alpha)\rangle_s f_A)_{T_{NI}} \quad (9)$$

and plotting the quantity on the left-hand side against the quantity on the right-hand side (Fig. 9), reveals a positive departure from the behavior predicted assuming a uniform distribution of binding sites. This is consistent with a preference for sites with the smaller radius of curvature which are those having the higher charge densities. These results could be used as a test of models for ion condensation[52,53] on ellipsoidal micelles. What makes these results interesting is that the variation of f_A with temperature (Fig. 8) reflects that of the axial ratio a/b [Fig. 3(b)]. That is, increase of f_A on lowering the temperature is a consequence of the growth and associated change in surface charge density of the micelle; it is not the cause of this growth, merely the effect.

IV. CONCLUSIONS

The phase behavior, in particular the occurrence of the tricritical point at which the nematic to lamellar transition crosses over from second to first order behavior, and the temperature dependence of the nematic order parameter are consistent with sequential order–disorder transitions in a system of discoidal micelles. The transition from the discotic nematic to the discotic lamellar phase is therefore envisaged as simply involving the propagation of a one-dimensional density wave along the nematic director. The x-ray scattering patterns are indicative of the buildup of fairly extensive short range lamellar-like correlations (pseudolamellar clusters) in the nematic phase as the transition to the lamellar phase is approached. This behavior is reminiscent of thermotropic calamitic nematics where the *cybotactic clusters*[54] correspond to the pseudolamellar clusters of the micellar system. In contrast to thermotropics, the micelles appear to undergo relatively independent, reorientational fluctuations in the nematic phase, at least in the vicinity of the transition to the isotropic phase; behavior consistent with the low packing fraction of the micelles. The micelles grow on cooling, partly as a consequence of the effect of temperature, but more so, as a result of a coupling behavior between the micelle structure and the incipient order of the nematic and lamellar phases. This has the effect of compressing the temperature range of the nematic phase.

These new results for the APFO system are supportive of and more definitive than our earlier results for the CsPFO system.[7,14,15] The phase diagrams for both systems are very similar when plotted in T vs ϕ coordinates, except that corresponding transitions are some 23 K higher for the CsPFO system. Both systems exhibit discotic lamellar phases and tricritical points. The TMANFN system has been reported[26] to form a discotic lamellar phase and it is quite possible that a detailed study of its phase behavior would reveal a tricritical point. Thus, the experimental observations for these short chain fluorocarbon soaps is not consistent with the notion[17] of a transition from a discotic nematic phase to a classical lamellar phase in which the bilayers are perforated by microscopic defects. However, the classical bilayer must be the limiting low temperature structure. A transition to such a phase is therefore expected on cooling, but it is not detected in either the APFO or CsPFO systems due to the intervention of crystallization. Perhaps the behavior of the system could be modulated by additives to render such a transition possible.

To conclude, it has been demonstrated that discoidal micelles can undergo nematic to smectic-A-like transitions, it now remains to be seen whether canonic micelles can undergo similar transitions as recently demonstrated for systems of hard rods.[55]

ACKNOWLEDGMENTS

We wish to thank the Science and Engineering Research Council for project grants to NB and a studentship to DP. We also thank the Royal Society of London and the British Council for travel grants to, respectively, NB and KWJ and the University Grants Committee for a scholarship to MHS.

[1] B. Lindman and H. Wennerström, *Topics in Current Chemistry* (Springer, Berlin, 1980), Vol. 87, pp. 1–84.
[2] G. J. T. Tiddy, Phys. Rep. 57, 1 (1980).

[3] J. Charvolin and J. F. Sadoc, J. Phys. Chem. **92**, 5787 (1988).
[4] B. J. Forrest and L. W. Reeves, Chem. Rev. **81**, 1 (1981).
[5] W. M. Gelbart, W. E. McMullen, and A. Ben-Shaul, J. Phys. Paris **46**, 1137 (1985); W. E. McMullen, W. M. Gelbart, and A. Ben-Shaul, J. Chem. Phys. **82**, 5616 (1985); W. M. Gelbart, W. E. McMullen, A. Masters, and A. Ben-Shaul, Langmuir **1**, 101 (1985).
[6] M. R. Rizzatti and J. D. Gault, J. Colloid Interface Sci. **110**, 258 (1986).
[7] N. Boden, S. A. Corne, and K. W. Jolley, J. Phys. Chem. **91**, 4092 (1987).
[8] P. J. Photinos, L. J. Yu, and A. Saupe, Mol. Cryst. Liq. Cryst. **67**, 227 (1981).
[9] M. C. Holmes and J. Charvolin, J. Phys. Chem. **88**, 810 (1984).
[10] M. C. Holmes, J. Charvolin, and D. J. Reynolds, Liq. Cryst. **3**, 1147 (1988).
[11] M. J. Sammon, J. A. N. Zasadzinski, and M. R. Kuzma, Phys. Rev. Lett. **57**, 2834 (1986).
[12] N. Boden, K. W. Jolley, and M. H. Smith, Liq. Cryst. **6**, 481 (1989).
[13] W. L. McMillan, Phys. Rev. A **4**, 1238 (1971); **6**, 936 (1972).
[14] N. Boden, S. A. Corne, M. C. Holmes, P. H. Jackson, D. Parker, and K. W. Jolley, J. Phys. Paris **47**, 2135 (1986).
[15] M. C. Holmes, D. J. Reynolds, and N. Boden, J. Phys. Chem. **91**, 5257 (1987).
[16] N. Boden, S. A. Corne, and K. W. Jolley, Chem. Phys. Lett. **105**, 99 (1984).
[17] P. J. Photinos and A. Saupe, Phys. Rev. A **41**, 954 (1990).
[18] N. Boden, M. C. Holmes, D. Parker, and K. W. Jolley, Liq. Cryst. (to be submitted).
[19] P. J. Photinos and A. Saupe, J. Chem. Phys. **90**, 5011 (1989).
[20] M. R. Fisch, S. Kumar, and J. D. Litster, Phys. Rev. Lett. **57**, 2830 (1986).
[21] K. Fontell and B. Lindman, J. Phys. Chem. **87**, 3289 (1983).
[22] H. Hoffmann, Ber. Bunsenges. Phys. Chem. **88**, 1078 (1984).
[23] K. Reizlein and H. Hoffmann, Progr. Colloid Polym. Sci. **69**, 83 (1984).
[24] P. J. Photinos and A. Saupe, J.Chem. Phys. **84**, 517 (1986); **85**, 7467 (1986).
[25] G. Chidichimo, L. Coppola, C. La Mesa, G. A. Ranieri, and A. Saupe, Chem. Phys. Lett. **145**, 85 (1988).
[26] L. Herbst, H. Hoffmann, J. Kalus, K. Reizlein, and U. Schmelzer, Ber Bunsenges. Phys. Chem. **89**, 1050 (1985).
[27] G. J. T. Tiddy, Symp. Faraday Soc. **5**, 150 (1971); J. Chem. Soc., Faraday Trans. 1 **68**, 608, 653 (1972).
[28] P. G. DeGennes, Solid State Commun. **10**, 753 (1972).
[29] D. Brisbin, R. Dehoff, T. E. Lockhart, and D. L. Johnson, Phys. Rev. Lett. **43**, 1171 (1979).
[30] H. Marynissen, J. Thoen, and W. van Dael, Mol. Cryst. Liq. Cryst. **124**, 195 (1985).
[31] S. B. Rananavare, V. G. K. M. Pisipati, and J. H. Freed, Chem. Phys. Lett. **140**, 255 (1987).
[32] M. A. Anisimov, V. P. Voronov, A. O. Kulkov, V. N. Petukhov, and F. Kholmurodov, Mol. Cryst. Liq. Cryst. B **150**, 399 (1987).
[33] A. J. Leadbetter, in *The Molecular Physics of Liquid Crystals*, edited by G. R. Luckhurst and G. W. Gray (Academic, New York, 1979), p. 283.
[34] V_s is the partial molecular volume of the surfactant as calculated from the partial molar volume measured at 298 K. From measurements of the densities of solutions in the weight fraction w_S range 0.228 to 0.604, the partial molar volume of APFO and heavy water were found to be constant and equal to 230.5 and 18.01 cm^3, respectively (cf. 18.14 cm^3 for pure heavy water at the same temperature).
[35] The length l of a fluorocarbon chain from the terminal fluorine of the CF_3 group to the center of the α-carbon to carboxylate carbon bond is given by (Ref. 56) $l = 0.186 + 0.130N_C$, where N_C is the number of carbons in the fluorocarbon chain. The volume of the fluorocarbon core V is calculated from the volumes of the CF_3 and CF_2 groups obtained by fitting the density data of Skripov and Firsov (Ref. 57) for fluoroalkanes to the equation $V = 2V(CF_3) + mV(CF_2)$ where m is the number of CF_2 groups. The values are $V(CF_3) = 0.0884$ nm^3 and $V(CF_2) = 0.0381$ nm^3.
[36] N. Boden, S. A. Corne, K. W. Jolley, and D. Parker, J. Chem. Phys. (to be submitted).
[37] In the calculation of values for b the total volume of the micelle was calculated from $V_m = \tilde{n}[V(CF_3) + 6V(CF_2) + V(CO_2^-) + V(NH_4^+)]$. $V(CO_2^-)$ ($= 0.0474$ nm^3) was calculated from the difference in the volume of octanoic acid and the volume of the $CH_3(CH_2)_6$ group (Ref. 58) and $V(NH_4^+)$ ($= 0.0202$ nm^3) was calculated from the ionic radius of the ammonium ion. The calculated value of V_s using this method is 0.376 nm^3 while the value calculated from the partial molar volume is 0.383 nm^3.
[38] N. Boden, D. Parker, and K. W. Jolley, Mol. Cryst. Liq. Cryst. **152**, 121 (1987).
[39] C. Rosenblatt, Phys. Rev. A **32**, 1115 (1985).
[40] G. R. Luckhurst, in *The Molecular Physics of Liquid Crystals*, edited by G. R. Luckhurst and G. W. Gray (Academic, New York, 1979), p. 85.
[41] W. Maier and A. Saupe, Z. Naturforsch. Teil A **14**, 882 (1959).
[42] Y. Hendrix, J. Charvolin, M. Rawiso, L. Liebert, and M. C. Holmes, J. Phys. Chem. **87**, 3991 (1987).
[43] Y. Galerne and J. P. Marcerou, Phys. Rev. Lett. **51**, 2109 (1983).
[44] Y. Galerne, A. M. Figueiredo-Neto, and L. Liebert, Phys. Rev. A **31**, 4047 (1985).
[45] A. de Vries, J. Chem. Phys. **56**, 4489 (1972).
[46] L. W. Reeves and A. S. Tracy, J. Am. Chem. Soc. **96**, 365 (1974).
[47] H. M. McConnel and D. D. Thompson, J. Chem. Phys. **31**, 85 (1959).
[48] H. Fricke, Phys. Rev. **24**, 575 (1924).
[49] R. A. Robinson and R. A. Stokes, *Electrolyte Solutions*, revised 2nd ed. (Butterworths, London, 1980), Chap. 11.
[50] G. W. C. Kaye and T. H. Laby, *Tables of Physical and Chemical Constants*, 15th ed. (Longmans, New York, 1986).
[51] F. J. Millero, R. Dexter, and E. Hoff, Chem. Eng. Data **16**, 885 (1971).
[52] S. Engström and H. Wennerström, J. Phys. Chem. **82**, 2711 (1978).
[53] G. Gunnarssön, B. Jönsson, and H. Wennerström, J. Phys. Chem. **84**, 3114 (1980).
[54] A. de Vries, Mol. Cryst. Liq. Cryst. **10**, 31, 219 (1970); **11**, 361 (1970).
[55] D. Frenkel, H. N. W. Lekkerkerker, and A. Stroobants, Nature **332**, 822 (1988).
[56] P. H. Jackson, PhD. thesis, University of Leeds, 1980.
[57] V. P. Skripov and V. V. Firsov, Zh. Fiz. Khim. **42**, 1253 (1968).
[58] C. Tanford, J. Phys. Chem. **76**, 3020 (1972).